

Operational & Technical Design Aspects of Future Civil Rotary Wing UAVs

C. Sevin

Eurocopter Deutschland GmbH, Germany
Eurocopter, France

G-M. Saggiani

University of Bologna, Italy

P-M. Basset

ONERA, France

J-F. Boer

NLR, The Netherlands

Nomenclature

BES	Best Endurance Speed
BRS	Best Range Speed
CAPECON	Civil UAV Applications & Economic Effectivity of Potential Configuration Solutions
Ch	Hourly consumption
Ck	Kilometric consumption
Cs	Specific consumption
EC	Eurocopter
ECD	Eurocopter Deutschland GmbH
FCC	Flight Control Computer
GCS	Ground Control Station
GDT	Ground Data Terminal
LCC	Life Cycle Cost
M	Weight
MTBL	Mean Time Between Loss
NLR	National Aerospace Laboratory
ONERA	French Aeronautics and Space Research Center
RW	Rotary Wing
TOP	Take-Off Power
UAV	Unmanned Aerial Vehicle
UNIBO	UNiversity of Bologna
USICO	UAV Safety Issues for Civil Operations
W	Power
Zp	Pressure Altitude

0. ABSTRACT

This paper presents some main results of the coaxial rotor configuration design group of the EU funded CAPECON project. CAPECON [Ref. 1],

Presented at the 31st European Rotorcraft Forum, Florence, Italy, September 13-15, 2005.

launched by the European Commission in 2001, aims at providing civil UAV customers with cost-effective and safe configurations. Starting from a market survey, moving through the definition of two most promising multi-role missions using a matrix-method, the first part of the job ended with the definition of two operational concepts: these concepts were used as main requirements for the following configuration phase. Two rotorcraft configurations, a classical tail-rotor/main-rotor configuration and a coaxial configuration that matched the requirements, were chosen. The coaxial configuration was then sized and some work was performed on coaxial helicopter modelling in order to improve the performances prediction. At the same time, a Ground Control Station (GCS), for helicopter flight control and onboard payload data display, was developed. A preliminary Safety / Reliability calculation was also performed for Rotary Wing UAV Mission. Finally, a Life Cycle Cost (LCC) model was developed, including all parameters for the total operating cost of rotary wing civil UAVs. A matrix for the acquisition and operating costs of the UAV configurations was also established.

1. INTRODUCTION

Unmanned Aerial Vehicles (UAVs) are replacing manned aircraft for several military tasks and have the potential for a range of civilian roles. To investigate this potential for civil use and develop technologies and configurations for safe and cost effective civil UAVs, the CAPECON project was started May 2001. CAPECON is a European Framework program [Ref. 1] and part of the ex-ante cluster with USICO [Ref. 2] under the thematic network UAVNET.

In CAPECON 20 organisations (9 industries, 5 aeronautics and space institutions and 6 universities) from eight countries worked together. This paper describes some main results of the

coaxial rotor configuration work performed in the rotorcraft part of CAPECON. The partners involved in the rotorcraft work are listed in Table 1.

Table 1 CAPECON Rotorcraft partners

Name	Country
Agusta	Italy
Eurocopter	France
Eurocopter Germany	Germany
French Aeronautics and Space Research Center	France
German Aerospace Center	Germany
National Aerospace Laboratory	Netherlands
University of Bologna	Italy
Warsaw University of Technology	Poland

The rotorcraft work has been structured in a logical series of steps starting from the customers needs (applications) to design a system addressing these needs, see Figure 1.

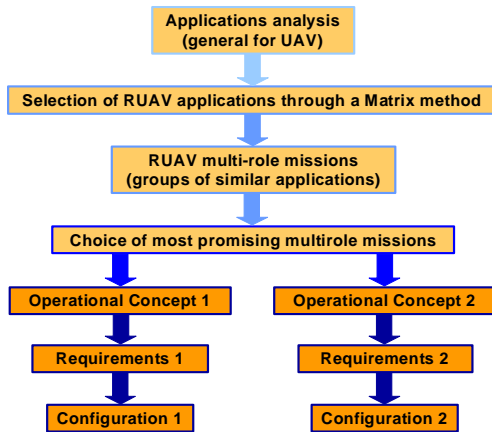


Figure 1. Configuration definition methodology.

Among the many applications foreseen for civil

rotorcraft UAVs are: local police surveillance, fire brigade assistance, and power line and pipeline monitoring and inspection. An overview of applications taken into account is given in Table 2.

Table 2 CAPECON applications

<i>Possible Use of Rotorcraft UAVs</i>
Snow and avalanche control
Catastrophic situation assessment
Volcanoes and eruption alert/research
Chemical and biological agent detection
Fire detection and pyromaniac deterrence
Interdiction of illegal hunting/border crossings
Low altitude search / kidnapping search support
Police chase vehicle for cars and/or people
Powerline monitoring and inspections
Dams and water reserves survey
Low altitude sea operation
Pipeline monitoring

For each of these applications, a standardised mission was constructed, which is top level description with just range, loiter time, maximum speed, operating altitude, payload sophistication level, safety requirement, and all-weather requirements. These standardised missions were grouped into a smaller number of multi-role missions.

The objective was to design two rotorcraft UAVs that can perform the two most economically beneficial multi-role tasks. These designs then have the best chance of becoming useful for civilian applications. The multi-role missions, which have been identified, are shown in Figure 2. A complete matrix method analytical study [Ref. 3] of multi-role missions was performed by the

	APP1 (Local surveillance)	APP2 (Search)	APP3 (Traffic Monitoring)	APP4 (Powerline+Pipeline)	APP5 (Agriculture)
RANGE (km)	50	200	150	200	20
ENDURANCE (h)	2	5	3	5	1
ALTITUDE (m)	100	500	300	100	10
PAYLOAD On Board Intelligence	2	4	3	5	2
All Weather Capabilities	YES	YES	YES	NO	NO
SPEED	LOW	HIGH	HIGH	MEDIUM	LOW
SAFETY	HIGH	MEDIUM	HIGH	MEDIUM	LOW
	Logical Concept 1	Logical Concept 2		Logical Concept 3	

Figure 2. Defined multi-role missions.

University of Bologna, Italy for CAPECON.

The two most promising multi-role missions, one dedicated to In-Line-of Sight missions (local missions) and the other to Out-of-Line of Sight missions (broader range missions), have been chosen for the configuration design phase. From there two operational concepts [Ref. 4, Ref. 5] were derived, describing two UAV Systems, a classical tail-rotor/main-rotor configuration for In Line of Sight Missions and a coaxial configuration for the Out-of-line of Sight Missions. The Operational Concept describes a large portion of the basic information on which a UAV system is based.

An important UAV cost driver is the sophistication level, which is driven to a large extent by the level of autonomy, see Table 3. The same applies to all weather capabilities.

Table 3 Onboard sophistication level

Level	Sophistication
1	Remotely Controlled (no SAS)
2	Stability Augmentation System (SAS)
3	Autonomous navigation
4	Some mission decisions
5	All mission decisions (fully autonomous)

Payload, performance and mission requirements derived from the operational concepts served as input for the sizing of the two configurations. The relatively small size of the two configurations required adjustment of the sizing model and a new engine model for small piston engines. For the coaxial rotor configuration, power required routines were developed and implemented, after investigation of the physical phenomena involved.

The sizing resulted in an elaborate pre-design of the coaxial rotor configuration UAV: geometry, inboard layout, weight breakdown, and the main performance parameters. After the actual sizing, a safety and reliability study was performed.

At the same time, a GCS (Ground Control Station), for helicopter flight control and payload data display, was developed. To test the GCS layout and the operator workload, the GCS was interfaced with a simplified coaxial rotor helicopter simulator, based on a FlightLab model developed by NLR (not presented here).

Finally, a Life Cycle Cost model was developed. A matrix for the acquisition and operating costs of all UAV configurations was established.

2. ROTARY WING UAV PRE-DESIGN

Modeling of the weight

As a first activity, EC performed a study on existing RW UAVs, to be able to adjust and validate Eurocopter's existing preliminary sizing model.

To adapt the empty weight calculation model, EC started from the general characteristics. For the main rotor for instance, we collected Rotor Diameter, Blade Chord, Number of Blades and Tip Speed data. When a parameter was unknown, an assumption was made, based on experience or observation. After that, the classical sizing model equations for the empty weight estimates were then adapted, and the output weight value of the sizing compared with the weight value provided by the UAV's manufacturer. This was done by adjusting sizing laws and technological coefficients with the available data.

The Table 4 shows some results from the weight calculation model.

Table 4 Weight calibration for UAV configuration (in kg)

	Heliot CAC Système	RPH-2 Fuji	Robocopter Kawada
Fuselage	54.69	36.95	103.51
Trains	10.32	7.85	16.63
Flight command	15.96	11.74	27.27
Blades	27.13	20.39	39.17
Hub	16.58	12.48	29.56
Transmissions	33.44	25.41	51.30
Engines	55.73	46.75	124.10
Fuel system	5.12	2.00	4.56
Internal equipments	0.00	0.00	0.00
Hydraulics	3.84	2.78	6.78
Electric circuit	15.84	11.44	27.96
Standard equipment	6.75	4.88	11.91
Mission equipment	0.00	0.00	0.00
Estimated empty weight	245.40	182.66	442.73
Real empty weight	230.00	205.00	499.00
Delta	6.28%	-12.23%	-12.71%

For the sub-systems sizing, some of the usual Eurocopter coefficients have also to be tuned so to take into account the relatively low weight of the aircraft. The following results are obtained with the modified tools.

Modeling of piston engines

Modeling of the mass

To adjust the Eurocopter sizing model concerning the weight of the piston engines, relatively to the output power, data was collected for both 2 and 4 stokes piston aviation engines. For each engine available, weight and power data were taken into account, always given at ISA/SL (International Standard / Sea Level) conditions.

The weight of an engine normally follows an empirical law. This means that a trend line can be established by plotting the dry weight of all piston aviation engines as function of their maximum power. More than 150 four stroke engines and 30 two stroke engines were considered.

The “trend lines” representing the collected data were calculated (Figure 3) to find equations that can be used in the EC sizing model. , one for two-stroke engines, valid for low power engines, and one for four-stroke ones, valid for heavier engines, but with an increased range of output power.

From this, the trend line equations, for weight vs. output power estimation, were derived:

Two-strokes engine: $M = 1.3703 W^{0.8505}$
 Four-strokes engine: $M = 3.0331 W^{0.7689}$

And the final sizing equation is:

$$M = 3.03\alpha W^{0.7689}$$

$\alpha = 1$ for a four-strokes engine (valid for an engine whose power does not exceed 300 kW)

$\alpha = 0.6435$ for a two-strokes engine (valid for an engine whose power does not exceed 130 kW)

With :

- M: engine weight (kg)
- W: maximum power (kW)
- α : technological coefficient

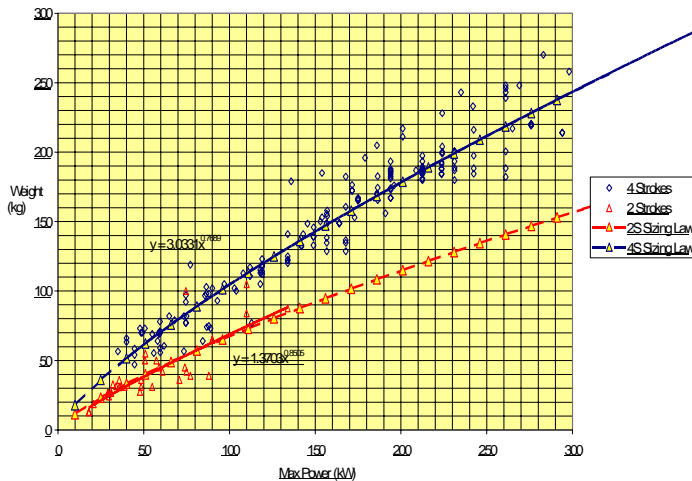


Figure 3 : Sizing Law (Weight vs. Power) for 4-strokes and 2-strokes engine

Modeling of the Power versus Temperature and Altitude

This study is mainly based on the Lycoming O360J, the Lycoming O320 and the Lycoming IO-540 all four-stroke turbo engines. The data were

provided by The Lycoming Company, USA [Ref. 6]. As they are extensively used in the aeronautics, they offer a good representation of aeronautical piston engines.

Power versus altitude

It is common to assume that the power evolves linearly as a function of the altitude, in standard conditions and at maximum continuous rating. This results in the following law:

$$W(Zp) = W_{SLISA} \cdot (\alpha Zp + \beta)$$

With

$$\alpha = -2.59 \cdot 10^{-5}, \beta = 1, Zp \text{ in ft, } W(Zp) \text{ in HP}$$

Power versus temperature

The variation of the power versus the air temperature is given by the following law:

$$W(T, Zp) = W(Zp) \times \sqrt{\frac{460 + T_s(Zp)}{460 + T}}$$

$$T_s(Zp) \cong -3,478 \cdot 10^{-3} Zp + 59$$

With

- T: real temperature in °F
- T_s(Zp): standard temperature in °F
- Zp: pressure altitude in ft
- W(Zp): Power in HP.

From there the equation of engine power versus temperature and altitude:

$$\frac{W(T, Zp)}{W_{SLISA}} \cong (-7,89 \cdot 10^{-6} Zp + 1) \times \sqrt{\frac{519 - 1,06 \cdot 10^{-3} Zp}{492 + \frac{9}{5} T}}$$

with T in °C, Zp in m and W_{SLISA} is the reference power at standard conditions (SL, 15°C).

Fuel consumption

Specific consumption C_S

The fuel consumption is given as function of the TOP (Take-Off Power, most of the time the only data given). It was estimated by use of the method of the previous paragraph.

It was found:

$$C_S = \frac{Ch_{TOP}}{W_{TOP}} = 578,7 \cdot W_{TOP}^{-0,2174} \text{ or}$$

$$Ch_{TOP} = 578,7 \cdot W_{TOP}^{0,7826}$$

With

W_{TOP} in kW C_s in g/h.kW C_h in g/h

Hourly consumption C_h function of the power

It can be observed that this law seemed to be linear, and moreover parallel for different engines. For this study, it has been used the same fuel consumption for two-stroke engine and for four-stroke engine.

The following law was found for a given engine, with the Hourly Consumption at Take-Off Power as only needed data.

$$Ch(W) = 0,2177.W + Ch_{TOP} - 1,1823.(Ch_{TOP} - 4,3498)$$

With

W in kW Ch in g/h

Mission requirements

From the definition of the operational concept, the mission envelope, to be covered by the UAV, was defined (Table 5). This provided a starting point for Helicopter sizing and performance estimation (like Max. Speed, Endurance, Ceiling, etc...).

	Civil Search	Traffic Monitoring	Powerline Monitoring
Ceiling	2100 m ISA+25°C	1300 m ISA+15°C	2100 m ISA+10°C
Max Speed	55 kts	100 kts	100 kts
Max Wind Speed	35 kts	35 kts	35 kts
Hover Out of Ground Effect (HOGE)	30 mn	20 mn	
Hover In Ground Effect (HIGE)			30 mn
Endurance	4 h at BRS	30 mn at BES	2 h at BRS

Table 5 Mission envelope used for sizing

Modeling of a coaxial configuration

After having modified EC’s sizing model for the UAVs (small rotorcraft), ECD obtained a first sizing concerning a conventional (single main rotor) configuration as a test case for tools assessment.

A second configuration [Ref. 7], a coaxial one, was then considered.

But at this stage, the tool was designed to size conventional configuration, with input dataset in accordance. To size a coaxial configuration, an

iterative process was used. An equivalent single main rotor helicopter was first sized. From there was derived the equivalent coaxial configuration.

For this purpose, some bibliographic research was performed, especially towards Russian papers, because of their experience with coaxial HC. By use of [Ref. 8], [Ref. 9] and [Ref. 10], it was managed to size a coaxial UAV which fulfilled the same requirements than the classical configuration.

The main adjustments were the reduction of the mean lift coefficient and the decrease of the main rotor diameter, for equivalent performances [Ref. 10]. An equivalent coaxial helicopter was expected to have maximum speed and BRS around 5% lower than an equivalent classical helicopter, but ceiling is about 17 to 21% higher [Ref. 10]. Those hypotheses were taken into account while performing the “classical equivalent sizing”.

The results of the sizing of ECD can be found in [Annex 1]. The next step was the estimation of the performance of the configuration.

3. PERFORMANCE ESTIMATION OF THE COAXIAL RW-UAV

From this first (quantitative) description, a more precise performance assessment has been performed with more refined models (developed in parallel during the pre-design phase). This modelling work is intended to verify the assumptions made during the pre-design phase and to improve the realism of the performances assessment. In particular, the key problem of the aerodynamic interferences between the two rotors of the coaxial configuration was addressed.

One of the ONERA contributions to the project was to develop an inflow model for coaxial rotors and to use it for the performances estimation. First, this interference model was formulated and set up within an analytical tool for the performance assessment by the energy method. Then in a second step, the new inflow model was implemented in a comprehensive non-linear rotorcraft flight mechanics simulation code that ONERA has adapted for the coaxial configuration.

Inflow model for coaxial rotors

For the sake of brevity, only the main features of the proposed coaxial model are here reported, while it is described with more details in an another paper [Ref. 11].

The model is dedicated to the calculation of the interference effect on the mean inflow through each rotor. In a first step, the swirl effect is neglected and the two extra interference downwashes ($v_{i1/2}, v_{i2/1}$) are determined by solving a system of two equations in which they are considered as additional inflows with respect to the mean inflow in the isolated rotor case (V_{i1}, V_{i2}). These two equations are based on the mass flow rate conservation and on the momentum conservation. The vertical separation (h) between the rotors is taken into account in the calculation of the contracted surface blown by the rotor 1 on the rotor 2. For that we used ONERA wind tunnel test showing the radial contraction of the rotor in function of the vertical distance below the rotor. In a second step, the effective induced flows through each rotor (V_{ile}, V_{i2e}) are calculated by using the interference inflows ($v_{i1/2}, v_{i2/1}$) as upstream conditions (as if each rotor was in climb or in a wind tunnel).

Then the model has been extended to the case of forward flights by accounting for the fact that the rotors wakes are skewed backwards which reduces the surface of interaction S' as illustrated on Figure 4.

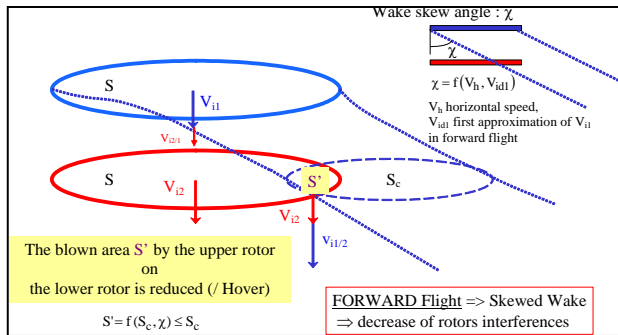


Figure 4 Extension of the model to the case of forward flights.

Furthermore, in forward flights it must also be taken into account that the rotors hub will have more drag than a classical main rotor hub. For performance calculation, this effect is accounted for by increasing the global drag power (P_f) by around 20 %. This value was estimated by validating our calculation tool in the case of an existing coaxial rotorcraft: the Kamov 32 for which the main performances are known (e.g. in the "Jane's book" [Ref. 12]).

Analytical estimation of the performances

The input data (Figure 5) in our performance calculation tool are based on the pre-design and sizing presented in the previous part.

Take-Off Gross Weight (kg) :	550	<i>Tip blade speed :</i>
Number of blades for each rotor :	2	U = 197,61 m/s
Rotor rotational speed (tr/min) :	740	
Blade average chord (m) :	0,17	<i>Calculated Average Lift Coefficient :</i>
Take-off power ISA/SL (kw) :	100	Cmoy = 0,46
Turbine (T) or Piston (P) Engine :	p	
Distance between the coaxial rotors (m) :	0,51	
Rotor Diameter (m) :	5,1	<i>Calculated Global Lift Force :</i>
Front Fuselage surface Sx (m²) :	0,615	Fm = 5611,3 N
Fuselage Drag coefficient Cd	1,05	

Figure 5 : Coaxial configuration data inputs.

First, for estimating the performances in hover and forward flights, the different sources of power consumption have been calculated w.r.t. the forward speed with analytical expressions based on the energy method and the interferences model. The power needed (P_n) is classically the sum of:

- P_i , the induced power ;
- P_D , the power due to the blade airfoil drag ;
- P_f , the fuselage drag power (all the sources of aerodynamic drag except those of the rotor blades airfoils).

On the other hand, the available power coming from the engine must be estimated taking into account the power losses through transmission, etc. (estimated here to 5%). P_u is the effective useable power. This power depends of course on the considered flight point in terms of altitude and temperature.

Unless specified differently, the performances are estimated here at $M=550$ kg and sea level in standard atmosphere conditions.

On this Figure 6, the induced power without interaction has also been drawn ("Pi no inter."). That corresponds to the induced power required by the two rotors without taking into account the interferences. It appears clearly that from hover until a forward speed around 75 km/h, the interferences increase the induced power compared with the case without interaction. Indeed above ~75 km/h, the wake skew angle is

such that the blown surface S' (see Figure 4) is null and thus there is no more significant interaction.

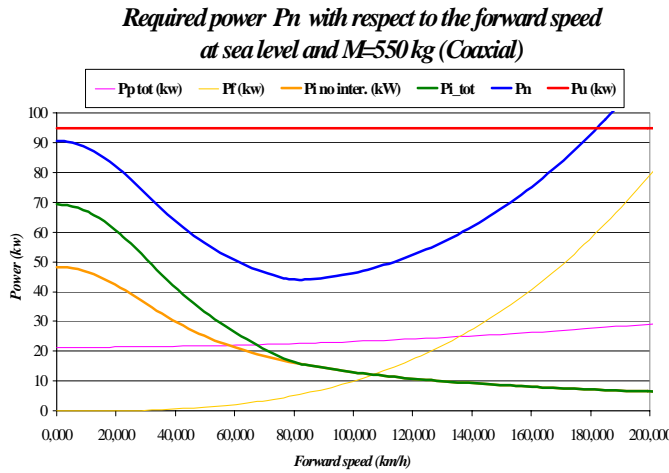


Figure 6 : Power assessment in forward flights for the coaxial.

The characteristic speeds: V_{be} (BES), V_{br} (BRS) and V_{max} (maximum speed), are assessed below.

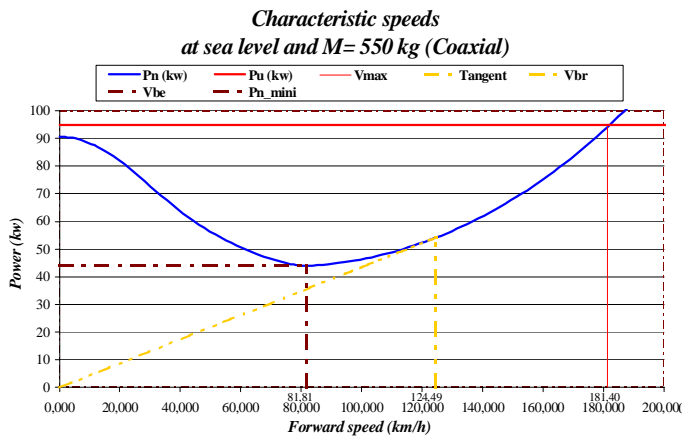


Figure 7 : Characteristic speeds assessment (coaxial $M=550$ kg).

From this analytical assessment, the results at sea level ISA for $M=550$ kg are:

$V_{max} \approx 181$ km/h, $V_{br} \approx 124,5$ km/h, $V_{be} \approx 82$ km/h

These results show (at least in terms of speeds) that even at the Max Take-Off Weight, the performances of the coaxial configuration are satisfying the mission constraints.

Performances assessment by flight mechanics simulation

The performance estimation by using a comprehensive flight mechanics simulation code will provide a better assessment of the performances. Moreover the adaptation of the simulation code for the case of the coaxial will prepare the work for further flight dynamics investigation.

Adaptation of the flight dynamics code

ONERA adapted the H.O.S.T. code ("Helicopter Overall Simulation Tool" e.g. [Ref. 13]) for the case of rotorcrafts with two coaxial contra-rotating rotors. This work is described more precisely in [Ref. 11]. In the present article, only the main lines are given.

➤ The airframe :

In absence of wind-tunnel test data giving the aerodynamic coefficients of the airframe, the fuselage is represented by the method of equivalent surfaces. These drag surfaces have been drawn from the CATIA design, (see 3D view in Annex 1 on Figure 15).

The additional drag due to the big hub in the coaxial case is accounted for by adding an extra drag force above the rotorcraft centre of gravity between the two rotors.

➤ The two contra-rotating coaxial rotors :

Both rotors are represented by a blade element model taking into account all the data description provided by the pre-design : chord, airfoil, ...

For the rotor induced velocity field, the user can choose among different model options (Meijer-Drees model or Pitt and Peters dynamic inflow model, etc.). For coaxial, the mean inflow through each rotor is calculated by the interference model developed by ONERA and which has been implemented within the flight dynamics code.

Power assessment with flight mechanics code

In the flight mechanics simulation code, the required power is not determined by the energy method, but by summing the consumed power to overcome the torques of the rotors. As mentioned, the performance estimation by the comprehensive simulation code is in principle more realistic because it computes the complete equilibrium of the rotorcraft. It turns out that the power curves and resulting characteristics speeds match well

between the two different tools and methods (analytical assessment with the energy method Figure 6, and numerical computation with the flight mechanics code Figure 8).

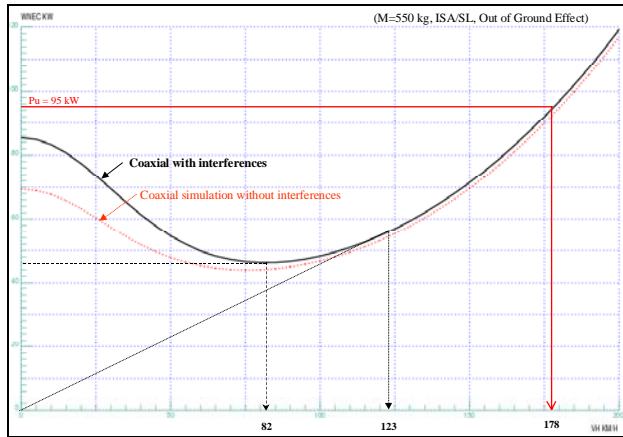


Figure 8: Flight mechanics code computation of the Power Needed for trim level flights, comparisons between the coaxial models (with and without interferences).

More precisely, in hover (Out of Ground Effect) :

- the analytical estimation gives :
 - without interaction : $P_n = 69.6 \text{ kW}$,
 - with interferences : $P_n = 90.6 \text{ kW}$.
- the flight mechanics simulations provides :
 - no interferences : $W_{nec} = 69.4 \text{ kW}$,
 - with interferences : $W_{nec} = 85.4 \text{ kW}$

The flight mechanics code assessment of the required power (with interferences) in hover is ~5kW lower than the analytical one. That may come from the fact that in the analytical calculation, the aerodynamic rotor interaction is taken into account only in the induced power assessment (P_i) and not for the blade airfoils drag power (P_p). In the comprehensive flight mechanics computation, the changes of the rotors inflow affect the blade local airspeeds and thus the blade airfoils angles of attack, which make vary their drag and the blade pitch control for trimming the rotorcraft.

In forward flight, it can be notice that the required power increases a little quicker with the forward speed in the computation by the flight mechanics code. For example with the analytical energy method assessment, the required power is around 90 kW at about 177 km/h, whereas with the flight mechanics calculation the 90 kW are required at 173 km/h. That could be due to the pitch attitude which becomes more and more negative for allowing the forward flights in the flight mechanics computation and thus the fuselage drag is

increased, compared with the analytical approximation where the pitch angle remains a flat null attitude whatever the forward the speed.

These results indicate that the model is realistic enough to provide the main tendencies. It takes into account the interferences at low speeds and their decrease with the increasing forward speed, as well as the extra drag of the coaxial hub which of course increases with the forward speed.

These modelling features allow validating the assumptions made in the pre-design phase. Indeed, the fulfilment of the mission requirements by the pre-design configuration has been verified by the more refined simulations.

4. SAFETY AND RELIABILITY

ECD performed a Functional Hazard Analysis (FHA) for RW UAV mission and operation.

The FHA covers the appropriate failure conditions and shows their criticality. It defines the safety objectives for the RW UAV according to:

- the Guidelines and Methods for Conducting the Safety Assessment Process on Civil Airborne Systems and Equipment;
- the Certification Considerations for Highly-Integrated or Complex Aircraft Systems;
- the Certification issued from the USICO European Project whose objective is to improve the safety of UAVs and enable their integration within civilian airspace.

Furthermore, the FHA shows the classification for the equipment concerning appropriate development assurance levels and software levels. This task was done by identifying the criticality of the RW UAV subsystems/equipment, by determination of common failure modes and subsequently by identification of which equipment had to be hardened against HIRF and lightning.

The potential failure conditions were identified and classified. Each equipment involved in an event as defined in the FHA was then listed.

All inputs/outputs of the RW UAV subsystems/equipment must be protected against environmental conditions, short circuits and polarity inversions. A malfunction of the described systems/equipment must not have influence to other systems/equipment installed in the helicopter. There must also be no HIRF influence to other systems/equipment. The final criticality and necessary redundancy of the equipments

have to be analysed in a System Safety Assessment (SSA).

For safety related consequences, some preliminary calculation concerning the MTBL, MTBUCL (Mean Time Between Uncontrolled Landing) and MTBCF (Mean Time Between Critical Failure) were done. It allowed improving the system, in order to reach the objectives, by adding a few redundancies. For reliability related consequences, some preliminary calculation concerning the MTBF (Mean Time Between Failure) were done.

Equipment description

The total system is made up of the equipment according to a minimum equipment list plus a mission payload. Hereafter, the basic equipment list for flying the UAV is given.

1. Air Vehicle

Effective airframe, capable of stable hovering with crash worthy fuel system and electrical generation with backup battery.

2. Control System

Redundant flight control computers ; FCC (to make it fly autonomously) ; data storage ; interfaces with GCS ; dual frequency data link with GCS and robust servo-mechanism and servomotors.

3. Navigation system

GPS (or a Differential GPS: DGPS) for the position ; Inertial Measurement Unit (IMU) with gyro and accelerometers to know the attitude and the velocity ; altimeter (IR or Radar or Sonar) ; dynamic and static pressure measurement ; compass and video camera for remote pilot flight control (better if digital to discern moving objects).

4. Safety Systems

Backup Micro-controller powered by the backup battery in order to fly back to the GCS in safe altitude if the primary FCC fails, or to autorotate if the engine has stalled ; safety pilot data link to allow manual control ; obstacle detection and anti-collision system (camera, radar, ultrasonic sensor) ; emergency process for engine shutoff and touch down with parachute.

A complete architecture diagram (Figure 9) illustrates this information.

The FHA allowed us to achieve the CAPECON safety requirement, sometimes by adding redundancies.

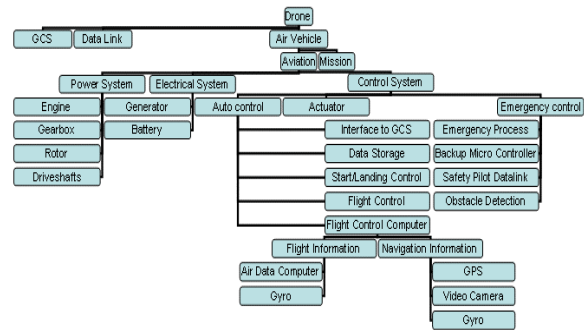


Figure 9: complete architecture diagram

The first result with the initial equipment list led to:

For safety related consequences:

- **Loss of the Aircraft:**
 $Q = 1,27 E^{-04} / FH$ (Mean Value)
Uncontrolled Landing:
 $Q = 1,39 E^{-04} / FH$ (Mean Value)

For mission reliability related consequence:

- **Interrupt of Mission:**
 $Q = 1,87 E^{-03} / FH$ (Mean Value)

After analysis of the result and identification of the most critical equipment, a redundant design of hydraulic supply pumps and DGPS in the navigation system led to the following results:

- **Loss of the Aircraft:**
 $Q = 2,7 E^{-05} / FH$ (Mean Value)
Uncontrolled Landing:
 $Q = 3,5 E^{-05} / FH$ (Mean Value)

All the results and details concerning the methodology can be found in [Ref. 14].

5. GROUND CONTROL STATION DESIGN

A GCS can be seen as the hub of the unmanned system, since it processes the data coming from the air vehicle and sends control instructions back to it. Indeed, a typical GCS will envelope at least three functions, that are mission planning, mission control and data manipulation. One of the UNIBO efforts in the project has been the design and development of the GCS for RWUAV mission planning and flight control.

At first, it was decided the GCS has to be able to operate the air vehicle in both autonomous or remote piloted flight mode and has to be transportable in a simple commercial van. But, since in the project there was no flying vehicle, it was then necessary to develop also an h/c simulator connected with the GCS: as a result a Mission Simulator Environment (MSE) was built (Figure 10) [Ref. 15].

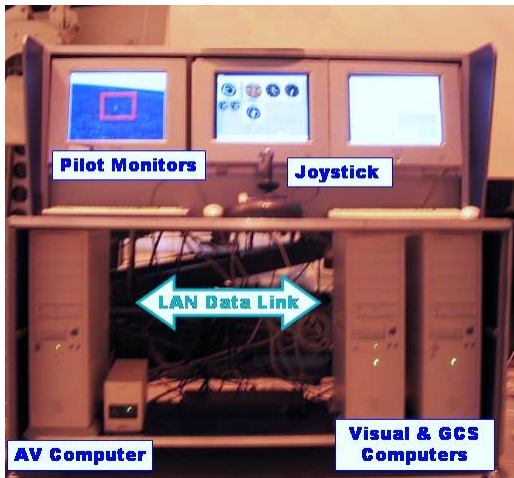


Figure 10 : UNIBO Mission Simulator Environment

A cluster of three computers and three TFT monitors composes this MSE and it can be divided in two main subparts:

- The H/C simulator, composed by 2 PCs (air vehicle PC and visual PC) and 1 monitor (visual screen).
- The GCS, composed by 1 PC and 2 monitors (virtual cockpit and mission control screen).

Regarding the h/c simulator, the air vehicle PC contains the Simulink dynamic model of the flying vehicle and the navigation guidance and control system while the visual PC contains the Visual System software that runs a 3D virtual view of the mission area (the left screen in Figure 12). The ground pilot can select three types of 3D virtual views: h/c external view, h/c pilot view and a view coming from a virtual payload (for example a slewable onboard EO camera). The terrain modelling is highly accurate as it is based on Digital Elevation Map data, with 3 arc-sec resolution, available from the US Geological Survey catalogue [Ref. 16].

The Simulink dynamic model is divided in several different blocks (Figure 11) and the main are:

- Two “communication” blocks for exchanging data with the GCS computer,
- The “helicopter dynamics” block which simulate the dynamics behaviour of the coaxial helicopter. The coaxial rotor model is base on the work performed by other partners [Ref. 17, Ref. 18]
- The Engine Governor block which changes the throttle settings in order to maintain constant rotor RPM,

- The Navigation, Guidance and Control System blocks which are able to provide controls for the air vehicle stabilization and enable the air vehicle to track a set of pre-planned flight segments, starting from any initial condition,
- the Switch block which is able to change the flight mode depending on a flag coming from the GCS,
- the Stability Augmentation System (SAS) & Autopilot block works both as stabilization and autopilot system. The autopilot gives proper control inputs to the “helicopter dynamics” block in order to maintain reference flight parameters defined by the GCS and depending on the selected flight mode.

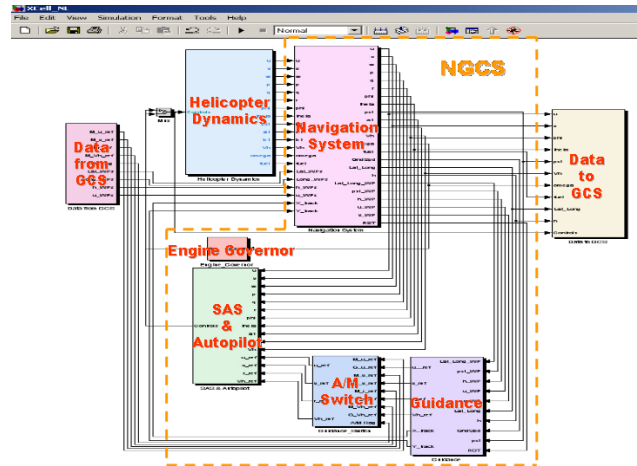


Figure 11 : Complete AV & NGCS Simulink model

The GCS Computer has two main tasks: it contains the GCS software and controls the information exchange among the other MSE computers.

The GCS software, developed with National Instruments Labview code, is able to:

- receive flight data form the a/v simulator PC and display it on the virtual cockpit screen (the central one in Figure 12);
- receive inputs from a joystick;
- allow the ground pilot to plan, re-plan and control the flight path using the mission planning monitor (the right one in figure Figure 12);
- send commands to the a/v PC according to the selected flight mode (autonomous or remotely piloted).

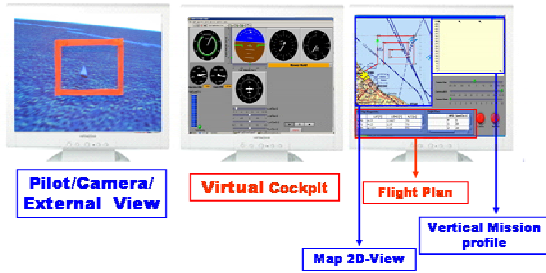


Figure 12 : GCS screens layout

Four different flight modes are available: manual, autonomous, acceleration and hover hold. The first is a joystick flight mode in which the joystick controls the h/c velocity vector (it is not a classical manual mode with collective, longitudinal and lateral cyclic control), while autonomous mode is a full automatic h/c flight using a pre-programmed flight plan. The other two modes are special cases in which it is required or a quickly h/c acceleration (acceleration mode) or to hover above a selected point (hover hold). All the flight modes can be selected by pushing a button on the joystick for a rapid flight mode change.

In order to evaluate the operational capabilities of the RWUAV, the developed configuration has been tested in an out of line of site “crashed aircraft” search mission. The air vehicle can take-off only in manual mode while the rest of the mission can be performed in autonomous mode following a pre-programmed flight plan (Figure 13). The ground operator can observe the searching area by means of a simulated gyroball camera, and, if something is found, he can switch into manual flight mode for better situation awareness. After a detailed survey of the aircraft crashed area, a simple push of the “back home” key on the joystick allows the air vehicle to return to the main base.



Figure 13 : Mission Scenario

As a result of the test case, the total fuel consumption for the mission was about 53 litres (Figure 14), that is less than the tank capability (72 litres). The consumption has been evaluated also in the worst case scenario (crashed aircraft at the end of the search area, plus ten minutes hovering and then flight back home) and the fuel consumption was about 68 litres.



Figure 14 : Mission Fuel Consumption

6. COSTS ANALYSIS AND RESULTS

Starting from a fixed-wing UAV cost model provided by IAI, ECD modified it for RW UAVs. The core of the cost model is based on LCC calculation, with an effort to reduce acquisition cost and operating & support cost, for example – design for manufacturing and reducing maintenance requirements through system design, by selection of reliable and durable components, all together will enable to reduce the LCC of the UAV system. The effort of reduction of LCC is a major task for the development team of each UAV system. This model is a parametric model based on the adjustment of military UAV programs costs to the civilian environment. The evaluation had to be performed by comparing the LCC of the UAV system for a life time of 20-30 years. Details and results can be found in Ref. 19.

LCC strongly depends on mission scenario - how many UAVs are needed to perform the mission, which will be defined by payload characteristics, UAV performance capabilities and UAV system reliability to perform the mission.

The following costing levels compose UAV System LCC:

- (a) Development cost, (b) Acquisition cost, (c) Initial support cost, (d) Operating and support cost and (e) Infrastructure cost.

Another main decision in LCC costing is to define the life cycle, in UAV systems, it is recommended to perform the calculation for 20 years, because a longer period usually involves system elements upgrading (such as electronics & software updating).

(a) Development Cost

Based on experience concerning the manned RW configurations, we defined the following data for the RW coaxial configuration:

- Theory (level 1) : 20 700 000 €
- Tests & Analysis (level 2) : 9 300 000 €
- Prototype (Level 3) : 7 000 000 € for 3
- Sum for development : 37 000 000 €

(b) Acquisition cost

It is composed of:

- (1) Acquisition of UAVs
- (2) Acquisition of GCS
- (3) Acquisition of GDT
- (4) Acquisition of payloads

The following paragraphs will describe in detail the composition of acquisition cost.

(1) UAV recurring cost

UAV recurring cost methodology is based on experience. It includes manufacturing cost, quality control cost. It depends of course highly of the quantity at production.

(2) GCS recurring cost

The study of the GCS and DL themselves were not in our scope of work. As it appears needed, UNIBO studied the ground support system technology. UNIBO has identified a set of possible solutions for the ground support system (which mainly includes the ground control station, the data link, the data distribution and the ground vehicle) for the configurations.

The results are really conservative. Without experience particularly in the field of satellite antenna, most information were found through internet, but the cost can probably be much lower. It was defined that for a specific RW UAV, 1 GCS is needed. Its cost is around 69 k€ for the coaxial configuration (including 1 van, 1 trailer, 1 generating set, 2 Notebooks; 1 joystick and 1 meteorological station).

(3) GDT recurring cost

It was defined that for a specific UAV wing, 1 GDT is needed. Its cost is around 310 k€ for the Coaxial configuration (including 2 Ku-Band Satcom Transceiver, 2 VHF Radio, 2 VHF Backup Radio, 1 GSM and 1 satellite phone).

(4) Payload recurring cost

It was assumed that payload cost was 50 k€, an arbitrary cost (usually defined by payload manufacturer).

(c) Initial Support Cost

• *UAVs initial support*

It includes mainly initial batch of spare parts, in order to be able to operate a UAV system. It is composed of a lot of items. At preliminary phase of program development it is assumed to be 20% of UAVs acquisition cost.

• *GCSs initial support*

Assumed equal to 20% of GCSs acquisition cost. *GDTs initial support*

Assumed equal to 10% of GDTs acquisition cost.

• *Payload's initial support*

There is no spare parts reservoir. In the case of a fault, payload is replaced (as LRU) by maintenance people, and sends for repair to the payload manufacturer.

• *GCE's initial support*

It was estimated (based on experience) that 2 sets of GCE are needed, and each set price is 0.4 m€. Usually the content list is long, and at program preliminary phase a gross estimation is performed. We had also to add guides for maintenance and system operating, and courses for operating and maintaining the system.

As an exemple, for a system made of 3 UAVs, 1 GCS, 1 GDT, 2 GCEs, 3500 pages of guides and 2000 hr of instruction, we reach the sum of 1,65 M€.

(d) Operating Cost

System operating cost is the larger part of life cycle cost. This estimation requires numerous assumptions reflecting the operation profile. It includes:

- Mission Scenario which has major impact on operating cost, since it defines how many UAVs are needed and how may UAVs are operated in order to perform the mission.
- Crew which strongly depends on maintenance manpower requirements.

UAV system maintenance goals and tasks are listed herein:

- Preventing maintenance
 - UAV phase inspection
 - Ground equipment annual inspection
- Corrective maintenance
 - UAV

- Ground equipment
- Operational tasks
 - UAV daily inspection
 - UAV Preflight Inspection
 - UAV Post-flight Inspection
 - Ground Equipment Pre-operational Check
 - Payload Reconfiguration
 - Turnaround
 - UAV Assembly

Each item in the above list should be translated to crew and time requirements for each maintenance task, for example: UAV preflight check will take 0.5 hours, by crew of 2 people. Typical crew requirements and labor rate (for the example of Coaxial RW UAV) were taken into account.

Other Expenses

Other expenses may include items like rent of vans, operating of generators, sleeping and food expenses per day per employee

Engineering and Communication Support

Operation of UAV systems requires engineering support (for mission performance and sub-systems support) and also communication support. Often it is desired to perform it with sub-contractors, in order to reduce the amount of fixed personnel stuff.

Inspection and Replacement of Major LRUs (line replacement unit)

In case of a standard UAV, the major LRUs are the engines. The Table 6 shows the expenses related to engines.

ENGINES INSPECTIONS	
Inspection every (flight hours)	500
Number of engines per UAV	1
Number of inspections/year	4
Labor hour per inspection/replacement	2.5
Acquisition per engine inspection	€500.00
Engine replacement every (flight hours)	2000

Table 6 Expenses related the engines

Inspection and Replacement of Other LRUs

At preliminary phase of the program, not all LRUs are known, it was assumed that 5% of UAV and GCS acquisition cost are yearly cost of spares and LRUs that are needed for normal operation of the UAV system.

Insurance

Five percent of acquisition cost of GCSs, and 5% of UAVs acquisition cost- are used for insurance rate. It should be calculated carefully, based on UAV MTBL.

Summary of Total Operating Cost

It is assumed that the UAV system will be operated for 20 year. The total operating cost for 20 years is estimated as operating cost per year, multiplied by 20. In order to simulate the inflation rate, the operating cost per year has been taken as 2%.

(e) Cost of Infrastructure

It is difficult to estimate the infrastructure cost of UAV system, because each customer has its own way to do it. Sometime the facilities are hired, and sometime investments are made in communication basis equipment as part of infrastructure cost, and etc' ...

It was decided that infrastructure cost will be in the range of 5%-10% of LCC cost.

We performed a parametric study, considering 500, 1000, 2000 and 4000 Flight Hours a year, production of 50 and 200 UAVs, and 1 or 2 UAV operated. We show Table 7 some of our results.

UAV System : 3 UAVs, 1 GDT, 1 GCS					
4000 FH with 2 UAV		200 UAV produced		50 UAV produced	
Operating cost per year	€ 500 104	% of	518 022	% of	
Years of operation	20	LCC	20	LCC	
Development	€ 979 305	6%	3 398 451	18%	
Acquisition	€ 1 941 196	12%	2 267 378	12%	
Initial Support	€ 1 657 239	11%	1 722 476	9%	
Operating	€ 10 002 077	64%	10 360 431	54%	
Infrastructure (7.50% of total)	€ 1 093 486	7%	1 331 155	7%	
TOTAL COST LCC	€ 15 673 303		19 079 891		
COST/FLIGHT HOUR [€/FH]	€ 196		238		
2000 FH with 2 UAV		200 UAV produced		50 UAV produced	
Operating cost per year	€ 355 122	% of	372 235	% of	
Years of operation	20	LCC	20	LCC	
Development	€ 979 305	8%	3 398 451	21%	
Acquisition	€ 1 941 196	15%	2 267 378	14%	
Initial Support	€ 1 657 239	13%	1 722 476	11%	
Operating	€ 7 102 436	57%	7 444 704	47%	
Infrastructure (7.50% of total)	€ 876 013	7%	1 112 476	7%	
TOTAL COST LCC	€ 12 556 189		15 945 485		
COST/FLIGHT HOUR [€/FH]	€ 314		399		
2000 FH with 1 UAV		200 UAV produced		50 UAV produced	
Operating cost per year	€ 412 398	% of	424 075	% of	
Years of operation	20	LCC	20	LCC	
Development	€ 979 305	7%	3 398 451	20%	
Acquisition	€ 1 941 196	14%	2 267 378	13%	
Initial Support	€ 1 657 239	12%	1 722 476	10%	
Operating	€ 8 247 954	60%	8 481 495	50%	
Infrastructure (7.50% of total)	€ 961 927	7%	1 190 235	7%	
TOTAL COST LCC	€ 13 787 621		17 060 035		
COST/FLIGHT HOUR [€/FH]	€ 345		427		
500 FH with 1 UAV		200 UAV produced		50 UAV produced	
Operating cost per year	€ 241 802	% of	252 876	% of	
Years of operation	20	LCC	20	LCC	
Development	€ 979 305	10%	3 398 451	25%	
Acquisition	€ 1 941 196	19%	2 267 378	17%	
Initial Support	€ 1 657 239	16%	1 722 476	13%	
Operating	€ 4 836 036	48%	5 057 513	38%	
Infrastructure (7.50% of total)	€ 706 033	7%	933 436	7%	
TOTAL COST LCC	€ 10 119 810		13 379 254		
COST/FLIGHT HOUR [€/FH]	€ 1 012		1 338		

Table 7 LCC cost & cost per Flight Hour

7. CONCLUSION

The main objectives of the CAPECON project were reached, by defining safe cost-effective, Civil UAV configurations. Particularly, the coaxial helicopter candidate solution met the safety, cost and performance design goals.

Acknowledgements

The authors would like to acknowledge the European Commission and the CAPECON consortium for allowing them to present this synthesis about a part of the RW UAV group work.

References

- Ref. 1 CAPECON Consortium, "Annex 1 Description of Work", CAPECON Project No. GRD1-2001-40162, Starting Date May 2002
- Ref. 2 USICO Consortium, "Annex 1 Description of Work", GROWTH Project No. GRD1-2001-40123, Starting Date May 2002
- Ref. 3 G.M. Saggiani, B. Teodorani, "Rotary wing UAV potential application: an analytical study through a matrix method" Aircraft Engineering and Aerospace Technology, Volume 76, Number 1 – 2004, pp 6-14.
- Ref. 4 Mouritsen, S.; Boer, J.F., "Operational Concept for Local surveillance UAV missions", CAPECON Project Internal Report, DLR & NLR, January 2003.
- Ref. 5 Basset, P.M., "ONERA Operational Concept for RW UAV non-local missions", CAPECON Project Internal Report, ONERA, January 2003.
- Ref. 6 „Detail Specification for Engine, Model IO-540-AE1A5 235 HP Direct Drive“, 8 November 2002 by the Lycoming company
- Ref. 7 Pretolani R., Saggiana G.M., Teodorani B., Internal Report on Definition of Rotary Wings UAVs Application and Configuration Selection“, University of Bologna, CAPECON Internal Report ID 3.2/1, June 2003.
- Ref. 8 25th European Rotorcraft Forum, Paper n° G22 "Coaxial Helicopter Rotor Design & Aerodynamics" By Boris Bourtsev, Sergey Selemenev, Victor Vagis, KAMOV Company, September 1999, Rome, Italy
- Ref. 9 "Phenomenon of a coaxial helicopter. High Figure of Merit at Hover." by B.N. Bourtsev, V.N. Kvokov, I.M. Vainstein, E.A. Petrosian, KAMOV Company, Liubertsy, Russia
- Ref. 10 V.A. Anikin, "Aerodynamics Features of a Coaxial Rotor Helicopter", KAMOV Company, USSR, ERF 1991
- Ref. 11 Basset, P.-M. : "Performances Comparisons of Different Rotary Wing UAV Configurations", 31st European Rotorcraft Forum, Florence, Italy, September 13-15, 2005.
- Ref. 12 "JANE'S ALL THE WORLD'S AIRCRAFT", Ninety-third year of issue, edited by Mark LAMBERT, London, 2002-2003.
- Ref. 13 Benoit B., Dequin A.-M., Basset P.-M., Gimonet B., Grünhagen W. von, Kampa K., "HOST, a General Helicopter Simulation Tool for Germany and France", American Helicopter Society 56th Annual Forum, Virginia Beach, Virginia, May 2 – 4, 2000.
- Ref. 14 Sevin,C., "Safety Concepts and Reliability Functional Hazard Analysis for Rotary Wing UAV Mission", ECD Report, 30.8.2003
- Ref. 15 Pretolani, R., Saggiani GM., Teodorani B., "Development of a mission simulation environment for Rotary Wing UAVs", CAPECON Project Report, UNIBO, May 2004
- Ref. 16 US Geological Survey catalogue <ftp://edcsgs9.cr.usgs.gov/pub/data/srtm/>
- Ref. 17 Jan-Floris Boer, Henk Haverdings, Martin Laban, "Co-axial rotor FLIGHTLAB simulations", CAPECON Project Report, NLR, December 2004
- Ref. 18 Pierre-Marie Basset, "Performance estimation and flight mechanics simulation", CAPECON Project Report, Onera, May 2004
- Ref. 19 C. Sevin, "Cost Model Database for Rotary Wing UAVS", CAPECON Deliverable D7/4, March 2005.

Annex 1

Rotary Wing Characteristics Checklist

Main parameters

Max Take-Off Weight	550. kg
Empty weight	330. kg
Fuel weight	70. kg
Payload weight	150. kg
Main Rotor Diameter	5.1 m
Main Rotor Chord	0.17 m
Main Rotor Blade Number	2*2
Main Rotor Blade Aspect Ratio	15
Main Rotor Solidity ()	0.085
Main Rotor Tip Speed	200 m/s
Main Rotor Nominal RPM	740 RPM
Fuselage Length	2.04 m
Helicopter Overall Length	5.1 m
Take-Off Power (kW)	100. kW
Disk Loading (@MTOW)	24.4 kg/m ²
Mean Lift Coefficient	0.28
Intra-rotor distance for coaxial (Hub Clearance)	0.51 m

Geometry

Three view drawings (Figure 15) with cross sections including:
 Main Rotor geometrical dimensions, Fuselage dimensions, C.G. location, Landing gear location

Surfaces breakdown

Wetted area	5,42 m ²
Sx Projected area in X direction	0,615 m ²
Sy Projected area in Y direction	1,576 m ²
Sz Projected area in Z direction	1,44 m ²
Main Rotor airfoil definition	Naca23012

Structural layout

Blades	Composite
Rotor Hub	Teetering Rotor
Fuselage	Al-Zn Alloy 2024
Housings	Al-Si-Mg Alloy
Main Gear Box	T B D
Engine	Centurion1.7TD TAE GmbH
Landing Gear	Aluminium

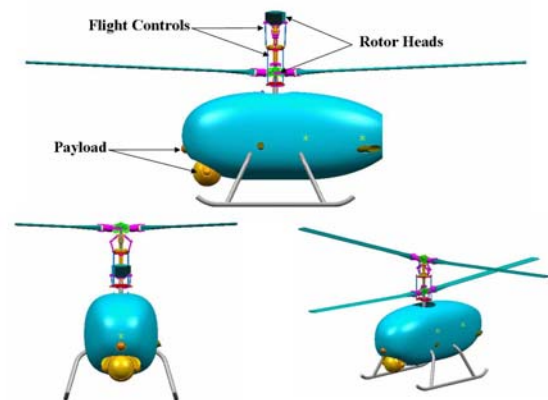
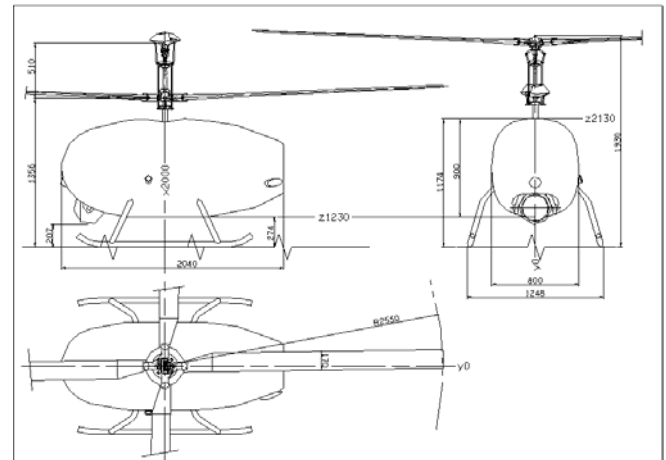


Figure 15 : 3-View drawings of the configuration



Figure 16 : Animation presented at the 2005 Paris Airshow